Fatigue Performance of High-Strength Pipeline Steels and Their Welds in Hydrogen Gas Service

Joseph Ronevich (Primary Contact),[a] Zhili Feng,[b] Andrew Slifka,[c] Robert Amaro,[d] Eun Ju Song,[a] Yanli Wang[b]
[a] Sandia National Laboratories (SNL)
[b] Oak Ridge National Laboratory (ORNL)
[c] National Institute of Standards and Technology (NIST)
[d] University of Alabama
7011 East Avenue
Livermore, CA 94550
Phone: (925) 294-3115
Email: jaronev@sandia.gov

DOE Manager: Neha Rustagi
Phone: (202) 586-8424
Email: Neha.Rustagi@ee.doe.gov

Project Start Date: October 1, 2015
Project End Date: September 30, 2018

Overall Objectives

- Enable the use of high-strength steel hydrogen pipelines, because significant cost savings can result by implementing high-strength steels as compared to lower-strength pipes.
- Demonstrate that girth welds in high-strength steel pipe exhibit fatigue performance similar to lower-strength steels in high-pressure hydrogen gas.
- Identify pathways for developing high-strength pipeline steels by establishing the relationship between microstructure constituents and hydrogen-accelerated fatigue crack growth (HA-FCG).

Fiscal Year (FY) 2018 Objectives

- Provide a comprehensive study of high-strength steel weld performance in high-pressure hydrogen gas by completing triplicate HA-FCG measurements in multiple high-strength alternate-consumable arc welds at constant hydrogen pressure, load-cycle frequency, and R-ratio = 0.5. (SNL/ORNL)
- Assess viability of lower-cost joining process for high-strength steels by completing triplicate HA-FCG measurements of friction stir weld at 3,000 psi, load-cycle frequency of 1 Hz, and R-ratio of 0.5. (SNL/ORNL)
- Define microstructure for an "optimized" high-strength steel suitable for pipeline use (i.e., a steel with targeted strength exceeding 100 ksi and HA-FCG similar to lower-strength steels). (SNL)
- Measure elastic-crack tip strains in representative compact-tension (CT) specimen in air and hydrogen and quantify dislocation accumulation at and near strained-crack tip in air and hydrogen (NIST). Calibrate cyclic large-scale plasticity model to measured crack tip strains, and perform parametric modeling study to determine the coupled load-rate and hydrogen diffusion-rate interactions.

Technical Barriers

This project addresses the following technical barriers from the Hydrogen Delivery section of the Fuel Cell Technologies Office Multi-Year Research, Development, and Demonstration (MYRDD) Plan[1]:

(D) High As-Installed Cost of Pipelines

(K) Safety, Codes and Standards.

Technical Targets

This project impacts the following technical targets for hydrogen delivery components from the Fuel Cell Technologies Office MYRDD Plan related to pipelines for gaseous hydrogen delivery:

- Total capital investment: 695,000 $/mile (FY 2020)
- Transmission pressure: 100 bar (FY 2020)
- Lifetime: 50 years (FY 2020).

Direct reductions in capital costs would be realized if higher-strength steels with thinner-wall pipes were permitted in ASME code (ASME B31.12 [1])

[1] https://www.energy.gov/eere/fuelcells/downloads/fuel-cell-technologies-office-multi-year-research-development-and-22

for hydrogen pipelines. Furthermore, understanding the performance baseline of high-strength welds in high-pressure hydrogen is necessary to gaining acceptance of high-strength hydrogen pipelines.

FY 2018 Accomplishments

- Completed at least two fatigue crack growth rate tests on four different high-strength X100 pipeline welds (W1, W3, W4, and a friction stir weld (FSW)). Tests were completed under 21 MPa hydrogen gas at 1 Hz and R=0.5, and results were compared to original X100 weld and lower-strength welds that showed only slightly higher fatigue crack growth rates (FCGR) in high-strength welds compared to lower-strength welds.
- Measured residual stresses in collaboration with University of California Davis on X100 weld and heat-affected zone, and published a paper in *Engineering Fracture Mechanics.*
- Examined influence of microstructure on HA-FCG based on gradient microstructures, microstructure orientation, and grain-size effects. Found that microstructure orientation has the largest (up to 5X) influence on HA-FCG compared to microstructure constituents and grain size (2X). This suggests that microstructural control of grain-boundary interfaces could affect HA-FCG performance in pipeline steels.
- Quantified elastic-crack tip strains as a function of distance in front of a crack tip in representative CT specimens. Measurements conducted in both air and 5.5 MPa pressurized hydrogen by use of Argonne National Laboratory's synchrotron X-ray source. Data collected were also used to determine dislocation density as a function of distance in front of the crack tip.
- Fatigue and fracture damage model was implemented in the finite-element code ABAQUS. The damage model predicts the onset of crack growth as a function of strain fields resulting from a crack tip.

INTRODUCTION

Steel pipelines represent an economical means of transporting gaseous hydrogen over long distances; however, it is well known that these carbon-manganese steels are susceptible to hydrogen degradation. Current steel pipelines codes (e.g., ASME B31.12 [1]) place limitations on higher-strength pipes due to the assumption that higher-strength pipes are more susceptible to hydrogen embrittlement than lower-strength grades. Recent testing [2–4] of pipeline steels with a range of specified minimum yield strength (SMYS) from 358 MPa to 689 MPa have not exhibited this trend and suggest that HA-FGR may not increase with strength. Given the recent results, the B31.12 code committee is reassessing the current limitations placed on higher-strength pipes, which would help reduce material and installation costs.

This project focuses on developing a pathway to enable the use of high-strength steel pipes. One means to accomplishing this goal is to assess the fatigue performance of high-strength steel pipelines under high-pressure hydrogen gas. The fatigue crack growth rate (da/dN) versus stress-intensity factory range (ΔK) relationship is a necessary input to structural integrity models applied to steel hydrogen pipelines. One specific assessment methodology for steel hydrogen pipelines is published in ASME B31.12 code [1], which requires testing of the base metal, weld, and heat-affected zone. One of the gaps is the fatigue performance of high-strength steel welds and whether the behavior will follow the same trends that the base metal exhibited over the SMYS range. The performance of the steel base metals or welds may vary as function of microstructure; therefore, development of physics-based relationships between FCGRs and microstructure would greatly enhance the structural integrity models and drastically reduce the test-burdening required to qualify materials for hydrogen use. The relationships between microstructures, contained in high-strength steels and welds, and hydrogen-assisted fatigue are evaluated in this study.

APPROACH

The objectives for this project are the following: (1) evaluate if girth welds in high-strength steel pipe exhibit fatigue performance similar to lower-strength steels in high-pressure hydrogen gas and (2) identify pathways for developing high-strength pipeline steels by establishing the relationship between microstructure constituents and HA-FCG. Based on these project objectives, the technical tasks are designed to furnish innovative high-strength steel products for evaluation and to measure performance metrics for these high-strength steel products (i.e., FCGRs under hydrogen gas) with high reliability. In this work, five different high-strength welds were examined to provide overall assessment of high-strength weld behavior in hydrogen. Included in this weld study was examination of a friction stir weld (FSW), an alternative that uses a non-consumable tool for welding, which provides a possible lower-cost joining option. Completion of these tasks will assist in reaching the goal of this work: the deployment of steel pipe with reduced wall thickness, which can lower costs for hydrogen pipeline installation.

RESULTS

Rate tests of HA-FCG were performed under 21 MPa hydrogen gas at R=0.5 and test frequency of 1 Hz for four high-strength pipeline welds. The welds were fabricated by ORNL using the same X100 base metal. Three different filler metals were used to fabricate welds: W1, W3, and W4. Additionally, an FSW was fabricated, which is an autogenous weld (e.g., no filler metal added). Test coupons were extracted from the center of each weld in the orientation such that the crack would extend radially outward through the wall. A minimum of two tests were performed for each weld as well as the heat affected zone of the FSW and X100A welds. The results are shown in Figure 1 for the high-strength welds compared to previously tested lower-strength welds. The results show some variability in the FCGR of the higher-strength welds; however, collectively, the higher-strength welds exhibit slightly higher FCGR compared to the lower-strength welds. The red dashed line in Figure 1 represents the ASME B31.12 design curve [6], which was recently approved for design of steels up to SMYS of 70 ksi and pressures of 21 MPa. The results show that most of the weld data fall below this design curve, which suggests potential use of these higher strengths in the future.

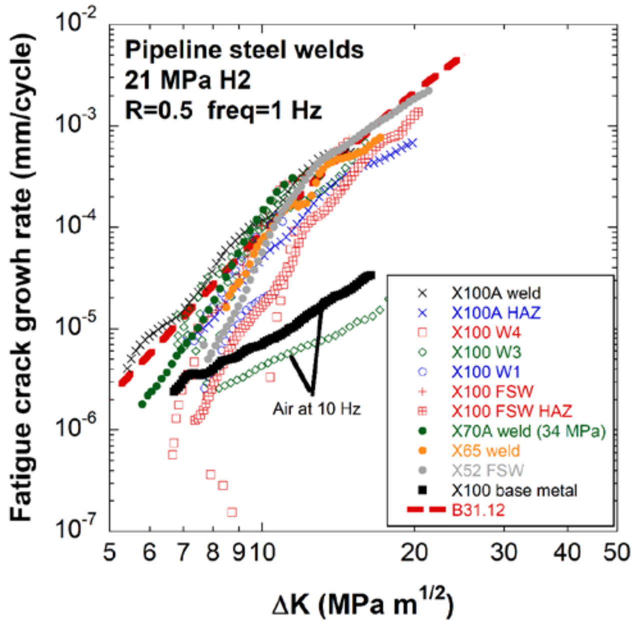

Figure 1. FCGR (da/dN versus ΔK_{app}) curves for high-strength pipeline steel welds compared to low-strength welds tested in 21 MPa H_2 gas. Tests performed in air at 10 Hz are shown for comparison along with B31.12 curve.

Residual stresses can be quite large in welds, particularly higher-strength welds; therefore, measurements of residual stress were conducted in collaboration with the University of California Davis to determine their magnitude and effect on FCGR. Figure 2a shows the residual stress influence on stress intensity factor (K_{res}) for duplicate measurements of the high-strength welds. Using the K_{res}, the FCGR curves were corrected such that the influence of residual stress was removed. The corrected FCGR curves (da/dN vs ΔK_{corr}) shown in Figure 2b exhibit a slightly narrower band compared to the raw data shown in Figure 1. The results suggest that higher-strength welds exhibit a range of FCGRs that are only slightly higher compared to lower-strength welds. Note that the residual stress was not measured on lower-strength welds.

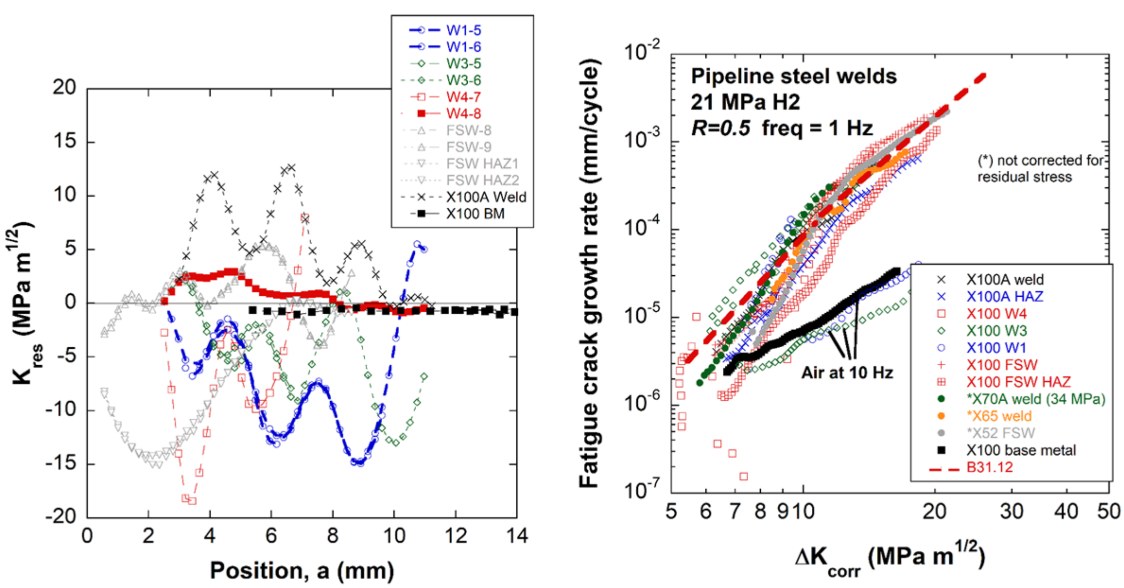

Figure 2. (a) Residual stress effects on K (e.g., K_{res}) as a function of position for high-strength steel welds. (b) FCGR curves for high-strength welds tested in 21 MPa hydrogen gas corrected for residual stress.

A Gleeble sample was fabricated and residual stresses were removed through a 2% rolling reduction on the sample. A constant ΔK test was performed at 10 MPa $m^{1/2}$ at R=0.5 and 1 Hz. The FCGR results are shown in Figure 3a. Microscopy was performed on select regions that demonstrated variations in FCGR as shown in Figure 3a. Region A consisted of coarse ferrite/bainite, region B was fine ferrite/bainite, and region C was ferrite/martensite. It is clear from the microscopy that the regions contained significantly different microstructural features, yet the difference in da/dN was less than a factor of 2, which suggests that the microstructural constituents examined have a small effect on FCGR.

The role of grain size and orientation of crack propagation were examined on X60 and X100 steels. The as-received X60 steel microstructure consisted of equiaxed 7-μm grain-size polygonal ferrite that was isotropic in nature, as shown in the inset image of Figure 3b. Tests were performed in T and R directions, which showed very similar FCGR in a hydrogen environment. The sample was heat treated at 1,100°C for 2 h to obtain a microstructure of 70-μm grain size. Tests were performed in the T direction and compared to the finer grain size. The coarse (70-μm) material exhibited slightly lower FCGR at lower ΔK and slightly higher FCGR above ΔK = 10 MPa $m^{1/2}$. Overall, the differences observed with testing orientation and grain size were less than a factor of 2. The X100 steel consists of an anisotropic microstructure of bainite with finer grain size (e.g., features less than 1 μm). Specimens were tested in both the L and R orientations, as shown in Figure 3c. The microstructure was elongated, due to the rolling process, in the L orientation, which means that a propagating crack in the L direction would be parallel to the elongated features and a crack in the R direction would be perpendicular to these features. The resulting FCGR measurements were significantly different in the two orientations. The measured FCGRs were nearly 5 times slower in the R direction than in the L direction, which suggests that interfaces play an important role in controlling FCGR.

The elastic-crack tip strains in a CT specimen were measured as a function of distance in front of the crack tip and ΔK. The measurements were performed in air and 5.5 MPa hydrogen by use of a novel test apparatus created at NIST and at the high-energy X-ray source at Argonne National Laboratory. The data were then used to determine the spatial dislocation density in a CT specimen. Data were also used in conjunction with strain-controlled test results to calibrate a large-scale cyclic plasticity material deformation model implemented in the finite-element platform ABAQUS. In the absence of the ability to quantify plastic strains within the crack-tip plastic zone, the solutions of models having varying crack-tip radii were compared to the measured strain solution. The CT-specimen strains resulting from a model having a blunted crack tip of 5-μm radius match the experimentally measured strains in the far field, so this work has provided sufficient evidence to support the use of a blunted crack tip, on the order of 5 μm, when modelling cracks in ABAQUS. Using this information, a fatigue and fracture-damage model has been implemented in ABAQUS. The damage model predicts the onset of crack growth as a function of strain fields resulting from a crack tip.

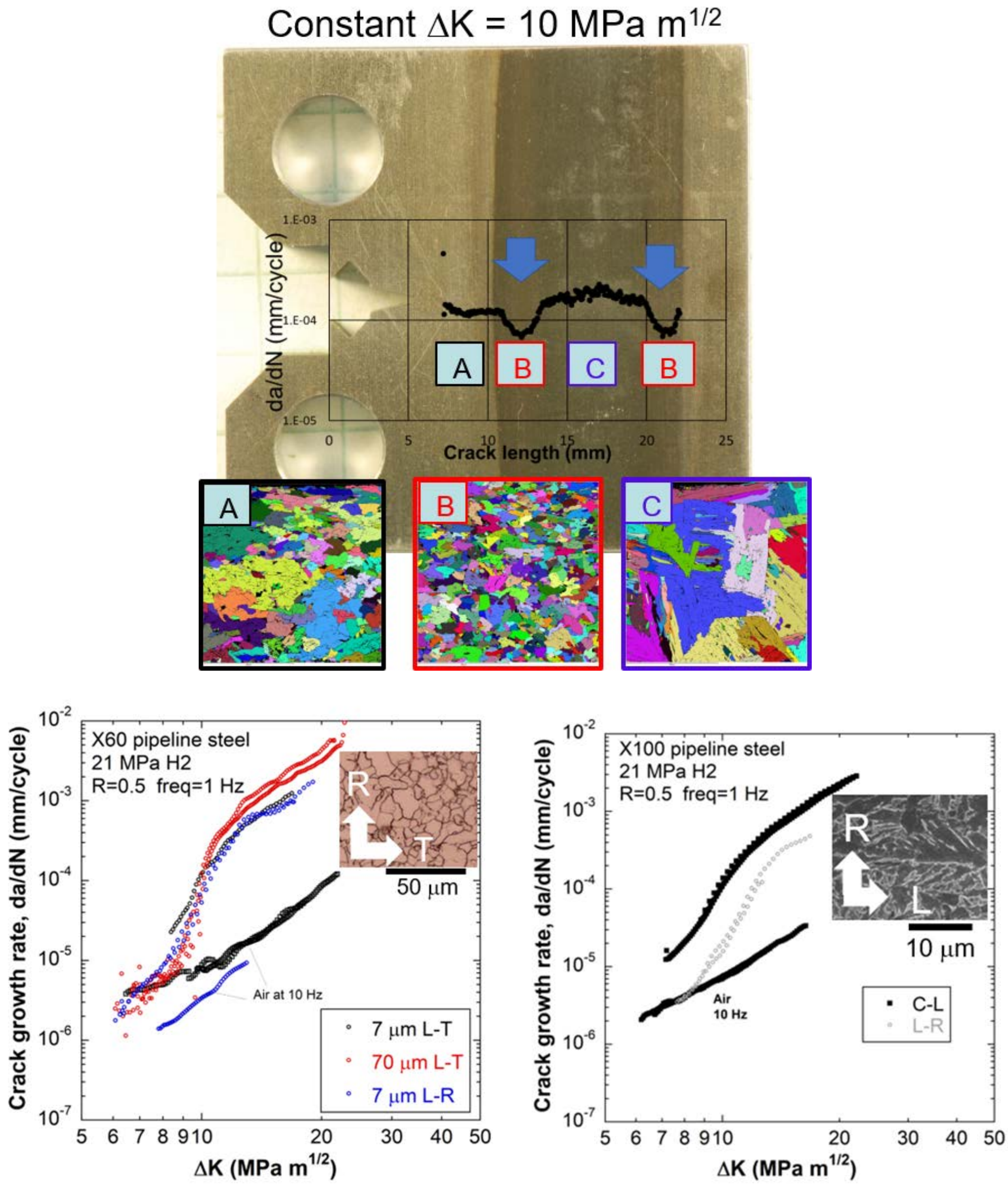

Figure 3. (a) Compact tension specimen with fatigue crack growth rate curve overlaid to show changes in da/dN as a function of microstructure. Region A consisted of coarse ferrite/bainite, region B consisted of fine ferrite/bainite, and region C consisted of ferrite/martensite. (b) da/dN curves of X60 pipeline steel in 21 MPa hydrogen showing differences in FCGR with grain size (7 and 70 μm) and orientation (L-R vs L-T). (c) da/dN curves of X100 pipeline steel in 21 MPa hydrogen comparing differences in FCGR with orientation (L-R vs C-L).

Parametric studies were performed using the calibrated deformation model to determine the effect of crack extension-hydrogen diffusion interactions. Results of the first parametric study indicate that the differences in hydrogen diffusivities exhibited by the common microstructures found in pipeline and pressure-vessel steels were insufficient to cause an effect on HA-FCG. Specifically, the first study indicates that the rate of hydrogen diffusion to the crack tip was dominated by the rate of loading and frequency of loading of the crack tip rather than the individual microstructure diffusivities. Subsequent parametric studies were performed in which the steel matrix was saturated with hydrogen. This boundary condition is indicative of in-service conditions for carbon steels because the diffusivities are sufficiently high to fill the lattice trap sites within minutes or hours. The second study found that the rate of change of the hydrogen diffusion trends with the rate of change of crack extension (per cycle) for ΔK values below about 15 MPa-m$^{1/2}$ as shown in Figure 4. Once the ΔK values exceed about 15 MPa-m$^{1/2}$, the rate of change of hydrogen diffusion saturates and therefore lags behind the rate of change of crack extension (per cycle). The studies indicate that the rate of hydrogen flux to the front of a moving crack tip is driven by the crack-tip loading rate and not by the material diffusivity. As the loading rate increases, up to a critical value (about 15 MPa-m$^{1/2}$ per cycle), the rate of hydrogen flux to the crack tip also increases. Above the critical loading rate, the effect of the stress-driven hydrogen flux rate saturates. These results suggest that the transition in HA-FCG behavior exhibited by most steels at about 15 MPa-m$^{1/2}$ results from the interaction of FCGR and stress-driven hydrogen flux rates, and not from material diffusivity (for diffusivities found in pressure-vessel and pipeline steel microstructures). The results were compared for loading frequencies of both 1 Hz and 0.01 Hz. Ultimately, the combined results of the two parametric studies suggest that the rate of change of the crack-growth driving force is the primary indicator of HA-FCG morphology. These statements above are merely correlations, but the parametric studies from this project have provided the ability to explore these theories beyond what experimental testing can provide. For example, testing at very low frequencies or the effects of a wide range of diffusivities cannot easily be performed in a laboratory; but these simulations allow us to explore the effects on hydrogen to theorize the role that these variables have in hydrogen accumulation.

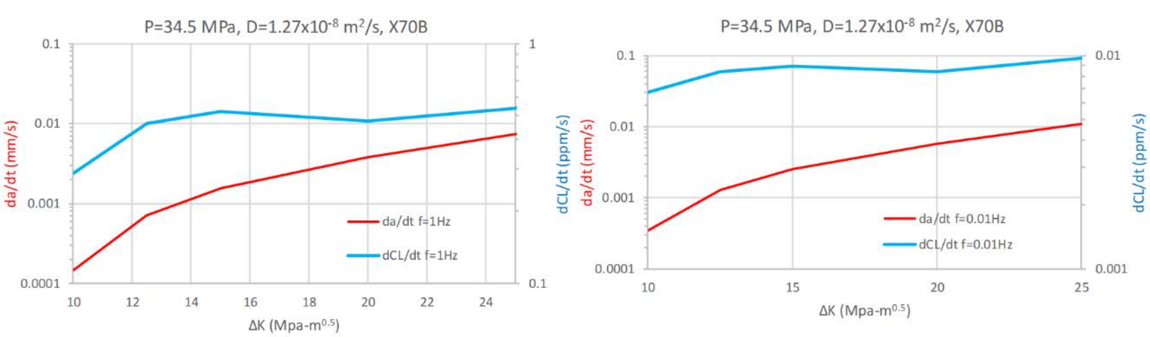

Figure 4. Results of parametric modeling study to determine the interaction between fatigue crack growth rate and hydrogen diffusion, as a function of applied ΔK and load frequency. Results indicate that the hydrogen diffusion rate saturates at an applied ΔK of ~15 MPa-m$^{1/2}$. Beyond this value of ΔK, the change in hydrogen diffusion rate no longer keeps pace with the change in FCGR. (a) Study results for load frequency of 1 Hz. (b) Study results for load frequency of 0.01 Hz.

CONCLUSIONS AND UPCOMING ACTIVITIES

- A comprehensive study of fatigue performance of high-strength pipeline steel welds was performed on five different X100 pipeline welds in high-pressure hydrogen gas. Variability in FCGR was attributed to residual stress in welds compared to the base metals. High-strength welds were observed to have only slightly higher FCGR compared to lower-strength welds, which suggests that higher-strength welded pipes could be used for hydrogen with proper design.

- (Future) One distinct gap that was identified was the lack of fracture-toughness data on pipeline welds. This is likely due to the challenges associated with extracting valid tests from localized regions. Sandia is planning to perform fracture testing on a variety of strength welds using carryover funds from this project in FY 2019.

- Laboratory-controlled microstructures were developed using a Gleeble and specialized heat treatments to examine the role of microstructural constituents, grain size, and grain orientation on susceptibility to HA-FCG. Of all the variables tested, microstructural orientation (e.g., induced from the rolling process) was observed to have the most dramatic effect on reducing HA-FCG. When the crack was oriented perpendicular to the rolling direction, HA-FCG was reduced up to 5 times compared to when the crack was oriented parallel to the rolling direction. This suggests that the role of interfaces (e.g., grain boundary) have a significant effect on suppressing HA-FCG.
- Elastic strain fields were characterized for the CT specimen crack tip as a function of ΔK, distance in front of the crack tip, and environmental conditions. Dislocation density was characterized for CT specimen crack tip as a function of ΔK, distance in front of the crack tip, and environmental conditions. A large-scale cyclic plasticity material model was implemented and calibrated to strain-field measurements in air. A crack initiation/extension damage model has been implemented in ABAQUS and calibrated to experimental results in air.
- (Future, as a function of ongoing work with the U.S. Department of Transportation) Large-scale cyclic plasticity material model to be calibrated to strain-field measurements in hydrogen. Crack initiation/extension damage model to be calibrated to experimental results in hydrogen.

SPECIAL RECOGNITIONS AND AWARDS/PATENTS ISSUED

1. R&D100 Award: Feng, Z., Yu, X., Wang, Y., David, S., Tzelepis, D.A., Gerth, R. J., Anderson, J., Douglas, J. "Filler Materials for Welding and 3D Printing."

FY 2018 PUBLICATIONS/PRESENTATIONS

1. J.A. Ronevich, C.R. D'Elia, M.R. Hill, "Fatigue crack growth rates of X100 steel welds in high pressure hydrogen gas considering residual stress effects," *Engineering Fracture Mechanics* 194 (2018): 42–51.
2. M. Connolly, P. Bradley, A. Slifka, D. Lauria, E. Drexler, "In situ synchrotron X-ray measurements of strain fields near fatigue cracks grown in hydrogen," *Materials Research Proceedings* 4 (2018): 17–22.
3. J.A. Ronevich et al., "Fatigue performance of high-strength pipeline steels and their welds in hydrogen gas service," Presentation at the DOE Hydrogen and Fuel Cells Program Annual Merit Review, Washington D.C., June 2018.
4. J. Ronevich et al., "Hydrogen Accelerated Fatigue Crack Growth of Multiple X100 Pipeline Steel Welds," International Conference on Metals and Hydrogen, May 29, 2018.
5. E.J. Song et al., "Correlating Steel Pipeline Microstructure to Fatigue Crack Growth Rates in High Pressure Hydrogen Gas," International Conference on Metals and Hydrogen, May 29, 2018.
6. E.J. Song, J.A. Ronevich, "Orientation dependence of hydrogen accelerated fatigue crack growth rates in pipeline steels," PVP2018-84835. Proceedings of ASME 2018 Pressure Vessel & Piping Conference, July 2018.
7. J. Ronevich et al., "Fatigue Performance of High-Strength Pipeline Steels and Their Welds in Hydrogen Gas Service," Hydrogen Delivery Tech Team meeting, February 28, 2018.
8. G. Rawls, J. Ronevich, A. Slifka, "Lowering costs of hydrogen pipelines through use of fiber reinforced polymers and modern steels," Fuel Cell Technologies Office Webinar, September 27, 2017.
9. J. Ronevich, R. Amaro, "Enhancing reliability and reducing costs of steels in hydrogen service through predictive computational modeling, advanced imaging, and high-pressure experimentation," Inter-agency Working Group presentation, April 17, 2018.

10. R.L. Amaro, C.P. Looney, M.J. Connolly, T.C. Cauthen, A.V. Woods, A.J. Slifka, "Parametric study of hydrogen diffusion in steel alloys through macroscopic and mesoscopic finite element modeling," 12th International Conference on Fatigue Damage of Structural Materials, September 16–21, 2018, Hyannis, MA.
11. C.P. Looney, Z.M. Hagan, E.S. Drexler, P.E. Bradley, A.J. Slifka, R.L. Amaro, "Modelling the test methods used to determine material compatibility for hydrogen pressure vessel service," 12th International Conference on Fatigue Damage of Structural Materials, September 16–21, 2018, Hyannis, MA.

REFERENCES

1. ASME. B31.12 Hydrogen Piping and Pipelines (New York, NY: ASME, 2011).
2. A.J. Slifka et al., "Fatigue crack growth of two pipeline steels in a pressurized hydrogen environment," *Corrosion Science* 78 (2014): 313–321.
3. J.A. Ronevich, B.P. Somerday, C.W. San Marchi, "Effects of microstructure banding on hydrogen assisted fatigue crack growth in X65 pipline steels," *Int. J. of Fatigue* 82 (2016): 497–504.
4. C. San Marchi, B.P. Somerday, K.A. Nibur, D.G. Stalheim, T. Boggess, S. Jansto, "Fracture Resistance and Fatigue Crack Growth of X80 Pipeline Steel in Gaseous Hydrogen," in ASME Pressure Vessels & Piping Division (Baltimore, Maryland: ASME, 2011).
5. J.R. Fekete, J.W. Sowards, R.L Amaro, "Economic impact of applying high strength steels in hydrogen gas pipelines," *International Journal of Hydrogen Energy* 40 (2015): 10547–10558.
6. ASME. B31.12 Hydrogen Piping and Pipelines (New York, NY: ASME, 2018 expected).
7. R.L. Amaro, E.S. Drexler, A.J. Slifka, "Fatigue crack growth modeling of pipeline steels in high pressure gaseous hydrogen," *International Journal of Fatigue* 62 (2014): 249–257.